



# Characterization and optimization of electron detachment dissociation Fourier transform ion cyclotron resonance mass spectrometry

Jiong Yang, Kristina Håkansson\*

Department of Chemistry, University of Michigan, 930 North University Avenue, Ann Arbor, MI 48109-1055, United States

## ARTICLE INFO

### Article history:

Received 25 March 2008

Received in revised form 24 May 2008

Accepted 27 May 2008

Available online 3 June 2008

### Keywords:

Electron detachment dissociation

Fourier transform ion cyclotron resonance

(FTICR)

Charge state

Oligonucleotide

Nucleic acids

## ABSTRACT

We have demonstrated that electron detachment dissociation (EDD) can provide extensive oligonucleotide backbone fragmentation, complementary to that of other MS/MS techniques. In addition, we have shown that, for oligosaccharides, EDD provides additional cross-ring fragments compared to collision-activated dissociation and infrared multiphoton dissociation. In our EDD implementation, the potential difference between a hollow cathode electron source and an extraction lens located in between the cathode and the ion cyclotron resonance (ICR) cell was crucial for successful fragmentation with changes as small as 0.2 V drastically altering fragmentation efficiency, a behavior that was not fully understood. Here, we present a detailed characterization of the electron current passing through the ICR cell as a function of this potential difference, the cathode bias voltage, extraction lens voltage, and the cathode heating current under EDD conditions. Our results show that the extraction lens voltage serves to regulate the number of electrons passing through the ICR cell. Thus, similar electron numbers passing through the cell can be obtained at low (1.2 A) and high (1.8 A) heating current as well as at different cathode bias voltages by adjusting the extraction lens voltage. This characteristic allowed us to investigate the influence of electron energy at fixed electron number and we found that optimum EDD efficiency was obtained with 16–22 eV electrons. We also investigated the influence of charge state on oligonucleotide EDD efficiency and sequence coverage and found that higher charge states provided improved data for a DNA 10-mer, presumably due to a more extended gas-phase structure.

© 2008 Elsevier B.V. All rights reserved.

## 1. Introduction

Tandem Fourier transform ion cyclotron resonance mass spectrometry (FTICR MS/MS) is widely used for biomolecular structural characterization [1–4]. Since the introduction of electron capture dissociation (ECD) in 1998 [5], many research groups have shown that ECD can provide unique fragmentation patterns for molecules as diverse as peptides and proteins [6], nucleic acids [7], polymers [8], lantibiotics [9], and siderophores [10]. ECD involves radical ion chemistry, resulting in more extensive peptide sequence coverage and retention of labile posttranslational modifications [11–13]. In 2001, Zubarev and coworkers introduced a new ion–electron reaction-based fragmentation method operating in negative ion mode; electron detachment dissociation (EDD) [14]. This technique provides unique fragmentation pathways for peptide dianions, including predominant C $\alpha$ –C backbone bond cleavage. Preferential cleavage of such backbone bonds over side-chain loss in EDD of peptides has been confirmed by ab initio calculations [15]. We

have extended EDD to oligonucleotide characterization and demonstrated extensive backbone fragmentation of oligodeoxy- [16] and oligoribo-nucleotides [17], complementary to that of other MS/MS techniques, such as collision-activated dissociation (CAD) and infrared multiphoton dissociation (IRMPD). Our group also showed that EDD can preferentially cleave C–S and S–S bonds in multiply charged disulfide-bonded peptide anions [18], retain higher order structure of DNA hairpins [19], and provide complementary cross-ring fragments for neutral and sialylated oligosaccharides [20]. Fabris and co-workers have applied EDD to oligonucleotide characterization and observed more extensive fragmentation compared to ECD [21]. Furthermore, Amster and coworkers found that EDD produces information-rich tandem mass spectra for glycosaminoglycans, including both cross-ring and glycosidic cleavage product ions [22]. The same group used EDD to distinguish the epimers glucuronic acid and iduronic acid in heparan sulfate tetrasaccharides based on diagnostic product ions, which are not observed in CAD or IRMPD [23].

In our previous EDD implementation [18] on a 7-T Bruker quadrupole (Q)-FTICR mass spectrometer equipped with an indirectly heated hollow cathode electron source [24], optimum fragmentation efficiency was observed at  $\sim$ –18 V cathode bias

\* Corresponding author. Tel.: +1 734 615 0570; fax: +1 734 647 4865.  
E-mail address: [kicki@umich.edu](mailto:kicki@umich.edu) (K. Håkansson).

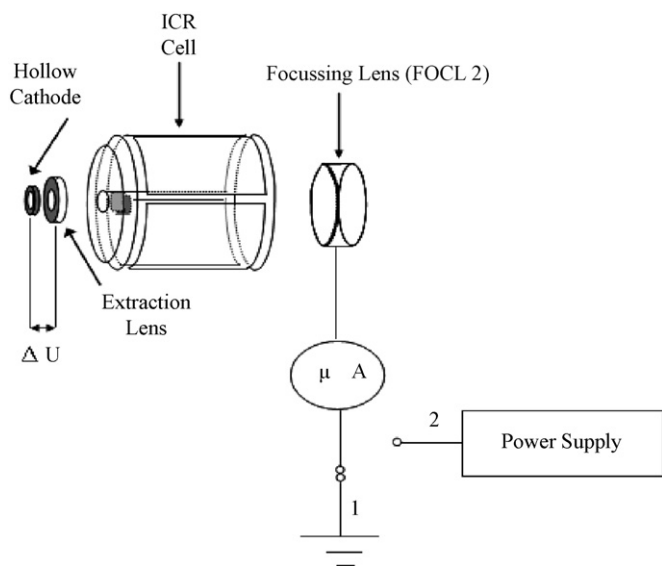


**Fig. 1.** Experimental configuration for electron current and energy measurements. The microammeter was connected to ground (1) when measuring electron current through the ICR cell, and connected to a floating power supply (2) when measuring the electron energy distribution.

voltage, an extraction lens voltage of  $\sim 19$  V, an irradiation time of 2 s, and a cathode heating current of 1.8 A (see Fig. 1 for a schematic drawing of this set-up). We found that precise tuning of the potential difference ( $\Delta U$ ) between the cathode and the extraction lens was crucial for successful EDD with an optimum around 1 V at 1.8 A heating current, which is the standard heating current used for ECD with the same instrument. Changes of  $\Delta U$  as small as 0.2 V drastically altered the EDD fragmentation efficiency, a behavior that we did not fully understand at that time. The more negative voltage on the extraction lens compared to the cathode at optimum EDD conditions suggests that so many electrons are emitted that space charge causes them to overcome this small retarding potential. Here, we present a detailed characterization of the electron current passing through the ICR cell as a function of the cathode bias voltage, extraction lens voltage, and cathode heating current in EDD. We also show characterization of EDD efficiency and sequence coverage as functions of precursor ion charge state and electron energy (the latter experiment being greatly facilitated by the insights gained from electron current measurements). Related experiments employing a different set-up for measuring electron current are presented by Amster and co-workers elsewhere in this issue [25].

## 2. Methods

### 2.1. Sample preparation

Reversed phase high performance liquid chromatography purified dA<sub>6</sub>, dC<sub>6</sub>, dT<sub>6</sub>, and d(CTATCAGTGA) oligonucleotide ammonium salts were purchased from TriLink BioTechnologies Inc. (San Diego, CA) and the peptide substance P (H-RPKPQQFFGLM-NH<sub>2</sub>) was from Sigma (St. Louis, MO). Negative ion mode electrospray solvent consisted of 1:1 (v/v) isopropanol:water (Fisher, Fair Lawn, NJ) with 10 mM ammonium acetate (Fisher). The final concentration of samples was 2–20  $\mu$ M.

### 2.2. Fourier transform ion cyclotron resonance mass spectrometry

All experiments were performed with a 7-T Q-FTICR mass spectrometer (Bruker Daltonics, Billerica, MA), which has been previously described [16]. The electrospray source was recently upgraded to include dual ion funnels (Apollo II electrospray ionization (ESI) source, Bruker Daltonics). For EDD fragmentation efficiency characterization, experiments investigating the role of precursor ion charge state were performed with the old ESI source (Apollo I, Bruker Daltonics) whereas all other experiments were performed with the new dual ion funnel source. The ESI flow rate was 70  $\mu$ L/h in both cases. EDD was performed with an indirectly heated hollow dispenser cathode electron source (Heat Wave, Watsonville, CA). The heater was set to approximately 8.5 V, generating a heating current of 1.8 A, unless specified otherwise. All mass spectra were acquired with XMASS (version 7.0.6, Bruker Daltonics) in broadband mode with 256 or 512k data points and summed over 20–30 scans. Data processing was performed with the MIDAS analysis software [26]: A Hanning window function was applied and data sets were zero filled once prior to fast Fourier transformation followed by magnitude calculation. Peak lists were generated and exported to Microsoft Excel for internal frequency-to-mass calibration with a two-term calibration equation. The calculated masses of the precursor ions and the charge-reduced species were used for calibration. Only assignments better than 20 ppm were included. EDD efficiency calculations were performed by dividing the total product ion abundance with the abundance of precursor ions prior to fragmentation. All abundances were normalized to their associated charge.

### 2.3. Electron current and energy measurements

Electron current and energy measurements were performed by measuring the electron current impinging on a floating cylindrical focusing element on the opposite side of the ICR cell, just outside the magnetic field (FOCL 2, see Fig. 1) with a digital multimeter (John Fluke, Everett, MA). For non-energy distribution measurements, the focusing element was grounded. An increase of the floating voltage to 20 V did not result in a significant current change thus, we believe that electrons were efficiently collected. The floating voltage necessary for performing the latter experiment, and for measuring energy distributions, was generated by a DC power supply (Goodwill Instrument, Taipei, Taiwan). Electron energy distributions were obtained by derivating the electron current with respect to the floating voltage.

## 3. Results and discussion

### 3.1. Electron current as a function of cathode bias voltage and extraction lens voltage

Our first series of experiments involved measurements of electron current passing through the ICR cell as a function of cathode bias voltage at fixed  $\Delta U$  (equal to 1 V). These experiments were motivated by our observation that EDD fragmentation efficiency and fragmentation pattern changed dramatically if the cathode bias voltage was increased from  $-18$  (the experimentally determined optimum) to  $-30$  V at fixed irradiation time and  $\Delta U$ . At higher cathode bias voltage, precursor ions were almost completely depleted but no product ions were observed. One possible explanation for this behavior is that product ions are too energetic (due to more energetic electrons) and are either ejected from the cell, or further fragmenting. However, an alternative explanation may be that there is a change in electron number as well as electron energy. Injection

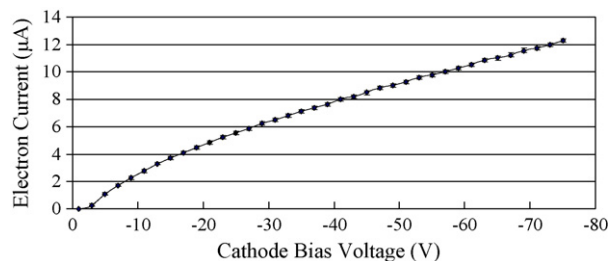


**Fig. 2.** Electron current through the ICR cell as a function of cathode bias voltage when  $\Delta U$  was kept constant (equal to 1 V). The cathode heating current was 1.8 A.

of too many electrons could cause space charge-related ejection of anions. Fig. 2 shows that the electron current through the ICR cell increases linearly in the cathode bias voltage range from  $-20$  to  $-80$  V. Thus, both the electron energy and electron number increase with increasing cathode bias voltage. By comparing the electron current at  $-18$  and  $-30$  V, it is evident that  $\sim 50\%$  more electrons are passing through the cell at the higher current, which is consistent with the second hypothesis above, i.e., too many electrons are generated, thereby causing space charge-driven anion ejection.

A second series of experiments involved measuring the electron current passing through the ICR cell as a function of the extraction lens voltage at fixed cathode bias voltage ( $-18.0$  V), as shown in Fig. 3. From this graph, it is seen that the electron current almost doubled when the extraction lens voltage was changed from  $-19.0$  (found to be optimum in our previous experiments [18]) to  $-18.8$  V. A change from  $-19.0$  to  $-18.8$  V, i.e., only 1 V, resulted in an eightfold current increase. Thus, the previously observed crucial influence of the extraction lens voltage in EDD can be clearly understood as this parameter serves to regulate the number of electrons passing through the ICR cell.

### 3.2. Electron energy distributions at EDD conditions

In order to better understand the EDD fragmentation process, it is desirable to determine the electron energy distribution in addition to the electron number and mean energy. Electrons emitted from an indirectly heated dispenser cathode are expected to have narrow energy distributions, which was also found experimentally (about 1 eV full width at half maximum) [27]. Fig. 4 shows the electron energy distribution measured in our instrument at a cathode bias voltage of  $-18.0$  V and extraction lens voltage of  $-19.0$  V (i.e., our previously determined experimental optimum). The distribution is narrow ( $<0.5$  eV) and the measured maximum was 0.7 eV lower than the applied cathode bias voltage. Similar measurements at cathode bias voltages of  $-8$ ,  $-10$ ,  $-12$ ,  $-14$ , and  $-16$  V performed at a  $\Delta U$  of 1 V showed that there is, on average, a 0.7 eV difference between the observed maximum of the energy distribution and the voltage applied to the cathode. Such reduction of the elec-

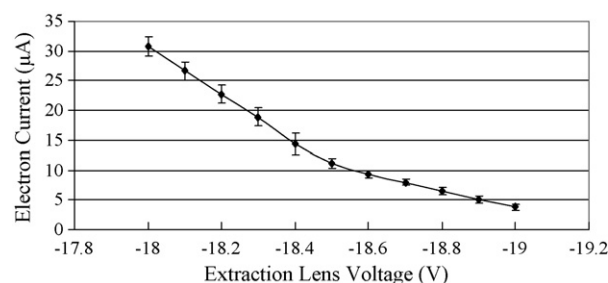


**Fig. 3.** Electron current through the ICR cell as a function of extraction lens voltage at fixed cathode bias voltage ( $-18.0$  V).

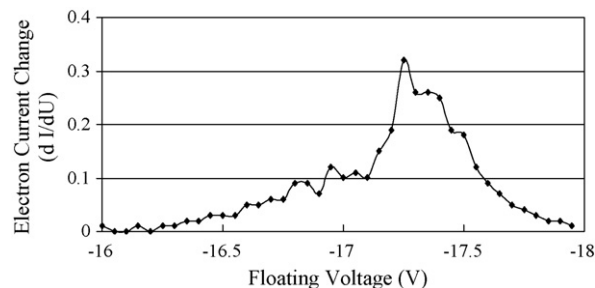


**Fig. 4.** Electron energy distribution at an applied cathode bias voltage of  $-18.0$  V and extraction lens voltage of  $-19.0$  V. The heating current was 1.8 A.

tron energy has been observed previously and was explained by the space potential of the electron beam [28].

### 3.3. EDD fragmentation efficiency as a function of cathode bias voltage at fixed electron current

From the experiments reported above, we found that two parameters change when the cathode bias voltage is changed; the electron energy and the electron current passing through the ICR cell. Thus, in order to measure EDD fragmentation efficiency as a function of electron energy alone, it is necessary to utilize parameters that provide a fixed electron number. Such experiments can be designed based on the data presented in Figs. 2 and 3: fixed electron current through the ICR cell is obtained by adjusting the difference between the cathode bias voltage and the extraction lens voltage, i.e.,  $\Delta U$ . Fig. 5 displays the experimentally obtained EDD fragmentation efficiency for the oligonucleotide dT<sub>6</sub> (top) and the peptide substance P (bottom) as function of cathode bias voltage at fixed electron current. These graphs show that the optimum EDD efficiency at fixed electron current (around  $4 \mu\text{A}$ ) is obtained at electron energies of 16–22 eV, i.e., significantly higher energy than, e.g., the ionization energy of phosphate anions (1.16–4.57 eV [29]); we proposed that deprotonated phosphate groups constitute the initial site of electron detachment in oligonucleotide anions [17]). However, it is well known from electron ionization of neutral organic molecules that the optimal energy is significantly higher (70 eV) than their ionization energy due to the inefficient energy transfer by electrons ( $\sim 10$ – $20$  eV are transferred to neutral

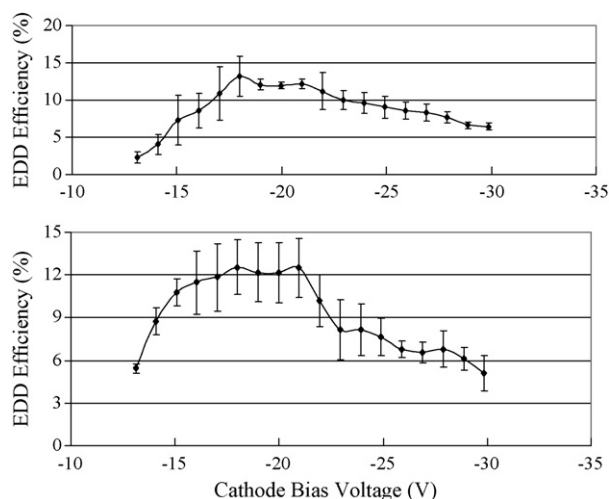


**Fig. 5.** EDD efficiency of the oligonucleotide dT<sub>6</sub> (top) and the peptide substance P (bottom) at different cathode bias voltages at fixed electron current ( $\sim 4 \mu\text{A}$ ). The optimum EDD efficiency was obtained at an electron energy of 16–22 eV.

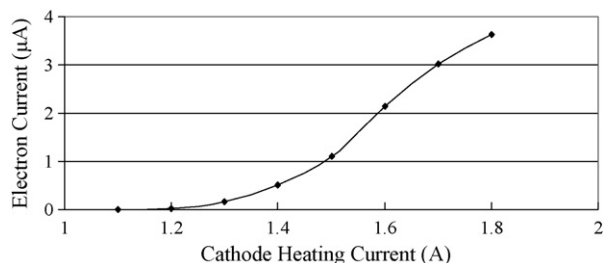


Fig. 6. Electron current passing through the ICR cell as a function of cathode heating current at fixed cathode bias voltage ( $-18.0$  V) and extraction lens voltage ( $-19.0$  V).

gaseous molecules during electron ionization [30], consistent with the quantum yield of ionization approaching unity at  $\sim 20$  eV [31]. In EDD, the targets are multiply negatively charged, thereby having lower electron binding energies due to intramolecular Coulomb repulsion [29]. A more speculative explanation for the optimum fragmentation efficiency at 16–22 eV may be that longer bond lengths exist in the vicinity of deprotonated sites such that the de Broglie wavelength of electrons ( $\sim 2.7$  Å at 20 eV) matches more closely at those energies.

#### 3.4. Can we perform EDD at lower cathode temperature?

As mentioned above, the recommended cathode heating current for ECD is 1.8 A (a temperature of around  $900^\circ\text{C}$  [27]). This high temperature may cause undesired heating of precursor ions that can result in thermally induced dissociation [32,33]. In order to minimize this problem, it would be desirable to perform EDD at lower cathode heating current. The data presented above in Figs. 2 and 3 suggest that it should be possible to compensate for the resulting lower electron number by adjusting  $\Delta U$ . In order to investigate this hypothesis, we measured the electron current passing through the ICR cell at different cathode heating currents at fixed cathode bias voltage ( $-18.0$  V) and extraction lens voltage ( $-19.0$  V). The results of these experiments are shown in Fig. 6. As expected, the electron current decreases dramatically with decreasing cathode temperature. At lower cathode temperature, insufficient numbers of electrons are generated from the cathode to allow efficient EDD. However, at a heating current of, e.g., 1.2 A, the same electron current ( $4 \mu\text{A}$ ) passing through the ICR cell can be obtained by changing the cathode bias voltage to  $-19$  V and maintaining the extraction

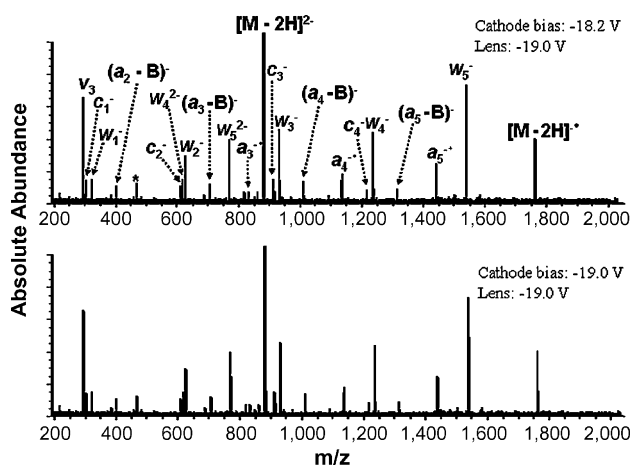


Fig. 7. EDD spectra (same scale) of the oligonucleotide  $dT_6$  at different cathode heating current: 1.8 A (top) and 1.2 A (bottom) but at fixed electron current passing through the ICR cell (\* = electronic noise;  $v_3$  = third harmonic).

lens voltage at  $-19$  V. At these conditions, the maximum of the electron energy distribution remains virtually unchanged (data not shown) compared to that observed at 1.8 A (Fig. 4). Fig. 7 shows EDD spectra from the oligonucleotide  $dT_6$  at cathode heating currents of 1.2 and 1.8 A, respectively, at the same electron current ( $4 \mu\text{A}$ ). Nearly identical EDD spectra were observed at these two settings, clearly demonstrating that control of the electron number passing through the ICR cell is crucial for successful EDD.

#### 3.5. The role of precursor ion charge state in EDD

Following ESI, we usually observe several charge states of macromolecular precursor ions of interest and have to decide what charge state to use for MS/MS experiments. Charge state plays a crucial role in both CAD/IRMPD and ECD [34–36] due to its influence on several factors such as ion stability, gas-phase structure, accessible kinetic energy, and electron capture cross-section. However, the

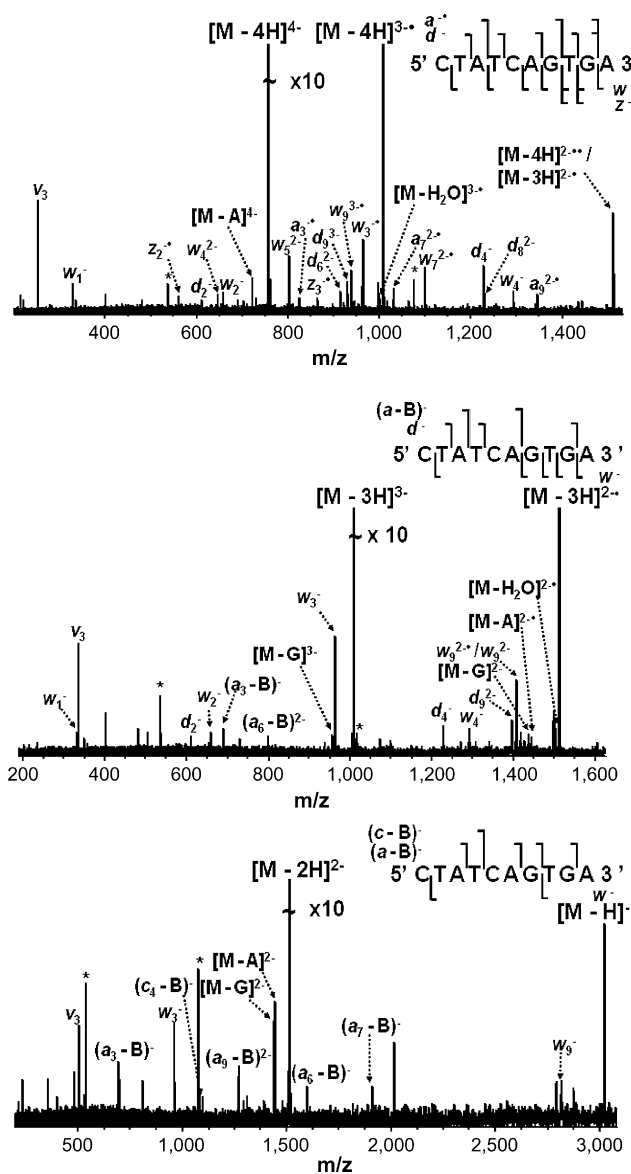


Fig. 8. EDD spectra from the quadruply (top), triply (middle), and doubly (bottom) deprotonated 10-mer oligonucleotide  $d(CATATCAGTGA)$  at a cathode bias voltage of  $-18.1$  V, an extraction lens voltage of  $-19.0$  V, and a cathode heating current of 1.8 A (\* = electronic noise;  $v_3$  = third harmonic).



**Table 1**  
EDD fragmentation efficiency of hexamer oligonucleotides at different charge states

Charge state	dA <sub>6</sub>		dC <sub>6</sub>		dT <sub>6</sub>	
	–2	–3	–2	–3	–2	–3
EDD fragmentation efficiency (%)	27	48	21	40	22	27

role of charge state in EDD has, to our knowledge, not been previously investigated. Table 1 shows the EDD fragmentation efficiency of the oligonucleotide hexamers dA<sub>6</sub>, dC<sub>6</sub> and dT<sub>6</sub> in their doubly and triply deprotonated states. These results show that higher EDD efficiency was obtained at the higher charge state although similar fragmentation patterns were obtained at both charge states.

Additional data were collected for a longer oligonucleotide: the 10-mer d(CTATCAGTGA), which was observed in three different charge states. Fig. 8 shows the EDD spectra obtained for the doubly, triply, and quadruply deprotonated forms of this oligonucleotide at the same experimental conditions. EDD of the 4-charge state (Fig. 8, top) resulted in extensive d and w-type product ions from backbone C–O bond cleavage [37] as well as several complementary radical a and z-type ions. The overall EDD efficiency was 35% and cleavage at all backbone interresidue bonds was observed. For the triply deprotonated 10-mer, fewer backbone cleavages were seen (Fig. 8, middle) compared to the 4-charge state and the EDD efficiency was lower: 16%. However, two (a – B)-type product ions (not observed for the 4-charge state) were detected. In EDD of the doubly deprotonated 10-mer, we found the most dominant product ions to correspond to (a – B)-type ions and only two w-type ions were observed. The EDD efficiency was further reduced to 5%. Thus, for this 10-mer, the amount of sequence information decreased drastically with decreasing charge state. An increase in negative charge could potentially decrease EDD efficiency due to Coulomb repulsion between anions and electrons (which can, e.g., result in poorer overlap between ions and the electron beam). However, for the relatively fast electrons involved, this effect seems minor. By contrast, the more unfolded conformations of higher charge states appear to result in the opposite effect, especially for longer chain oligonucleotides. This result is consistent with our previous data, which showed that EDD retains intramolecular interactions [16,19].

#### 4. Conclusions

This article demonstrates that the potential difference between the cathode bias voltage and the extraction lens voltage ( $\Delta U$ ) is a crucial parameter for successful EDD. The extraction lens voltage serves to regulate the number of electrons passing through the ICR cell. Optimum EDD efficiency at fixed electron current (around 4  $\mu$ A) was obtained at electron energies of 16–22 eV for the oligodeoxynucleotide dT<sub>6</sub> and for the peptide substance P. The electron current decreases dramatically with decreased cathode heating current. However, similar quality EDD can be achieved at lower heating current (1.2 A) by decreasing  $\Delta U$ . For oligodeoxynucleotides, the EDD efficiency and sequence coverage seems to increase with increasing precursor ion charge state.

#### Acknowledgments

This work was supported by the University of Michigan, a starter grant from the Petroleum Research Fund (43602-G6), and by a CAREER award from the National Science Foundation (CHE-05-47699). The authors would also like to acknowledge John Reves and Steve Parus from our electronics shop for their help with electron current measurements.

#### References

- [1] B. Bogdanov, R.D. Smith, *Mass Spectrom. Rev.* 24 (2005) 168.
- [2] K. Hakansson, H.J. Cooper, R.R. Hudgins, C.L. Nilsson, *Curr. Org. Chem.* 7 (2003) 1503.
- [3] S.A. Hofstadler, K.A. Sannes-Lowery, J.C. Hannis, *Mass Spectrom. Rev.* 24 (2005) 265.
- [4] Y.M. Park, C.B. Lebrilla, *Mass Spectrom. Rev.* 24 (2005) 232.
- [5] R.A. Zubarev, N.L. Kelleher, F.W. McLafferty, *J. Am. Chem. Soc.* 120 (1998) 3265.
- [6] R.A. Zubarev, D.M. Horn, E.K. Fridriksson, N.L. Kelleher, N.A. Kruger, M.A. Lewis, B.K. Carpenter, F.W. McLafferty, *Anal. Chem.* 72 (2000) 563.
- [7] K. Hakansson, R.R. Hudgins, A.G. Marshall, R.A.J. O'Hair, *J. Am. Soc. Mass Spectrom.* 14 (2003) 23.
- [8] B.A. Cerda, D.M. Horn, K. Breuker, F.W. McLafferty, *J. Am. Chem. Soc.* 124 (2002) 9287.
- [9] A.J. Kleinijnshuis, M.C. Duursma, E. Breukink, R.M.A. Heeren, A.J.R. Heck, *Anal. Chem.* 75 (2003) 3219.
- [10] H. Liu, J.Y. Lee, D.H. Sherman, K. Håkansson, *J. Am. Soc. Mass Spectrom.* 18 (2007) 842.
- [11] N.L. Kelleher, R.A. Zubarev, K. Bush, B. Furie, B.C. Furie, F.W. McLafferty, C.T. Walsh, *Anal. Chem.* 71 (1999) 4250.
- [12] K. Hakansson, H.J. Cooper, M.R. Emmett, C.E. Costello, A.G. Marshall, C.L. Nilsson, *Anal. Chem.* 73 (2001) 4530.
- [13] H.J. Cooper, K. Hakansson, A.G. Marshall, *Mass Spectrom. Rev.* 24 (2005) 201.
- [14] B.A. Budnik, K.F. Haselmann, R.A. Zubarev, *Chem. Phys. Lett.* 342 (2001) 299.
- [15] I. Anusiewicz, M. Jasionowski, P. Skurski, J. Simons, *J. Phys. Chem. A* 109 (2005) 11332.
- [16] J. Yang, J. Mo, J.T. Adamson, K. Håkansson, *Anal. Chem.* 77 (2005) 1876.
- [17] J. Yang, K. Håkansson, *J. Am. Soc. Mass Spectrom.* 17 (2006) 1369.
- [18] A. Kalli, K. Håkansson, *Int. J. Mass Spectrom.* 263 (2007) 71.
- [19] J. Mo, K. Håkansson, *Anal. Bioanal. Chem.* 386 (2006) 675.
- [20] J.T. Adamson, K. Hakansson, *J. Am. Soc. Mass Spectrom.* 18 (2007) 2162.
- [21] K.A. Kellersberger, D. Fabris, *Proceedings of the 53rd ASMS Conference on Mass Spectrometry and Applied Topics*, San Antonio, TX, 2005.
- [22] J.J. Wolff, I.J. Amster, L.L. Chi, R.J. Linhardt, *J. Am. Soc. Mass Spectrom.* 18 (2007) 234.
- [23] J.J. Wolff, L.L. Chi, R.J. Linhardt, I.J. Amster, *Anal. Chem.* 79 (2007) 2015.
- [24] Y.O. Tsybin, M. Witt, G. Baykut, F. Kjeldsen, P. Hakansson, *Rapid Commun. Mass Spectrom.* 17 (2003) 1759.
- [25] F.E. Leach, J.J. Wolff, T.N. Laremore, R.J. Linhardt, I.J. Amster, *Int. J. Mass Spectrom.*, 2008.
- [26] M.W. Senko, J.D. Canterbury, S. Guan, A.G. Marshall, *Rapid Commun. Mass Spectrom.* 10 (1996) 1839.
- [27] Y.O. Tsybin, M. Witt, G. Baykut, P. Håkansson, *Rapid Commun. Mass Spectrom.* 18 (2004) 1607.
- [28] B.S. Freiser, J.L. Beauchamp, *Chem. Phys. Lett.* 42 (1976) 380.
- [29] X.B. Wang, E.R. Vorpagel, X. Yang, L. Wang, *J. Phys. Chem. A* 105 (2001) 10468.
- [30] E. de Hoffmann, V. Stroobant, *Mass Spectrometry—Principles and Applications*, 3rd ed., John Wiley and Sons Ltd., West Sussex, England, 2007.
- [31] J. Berkowitz, *J. Phys. Essays* 13 (2000) 248.
- [32] M. Sena, J.M. Riveros, *J. Phys. Chem. A* 101 (1997) 4384.
- [33] R.L. Wong, E.W. Robinson, E.R. Williams, *Int. J. Mass Spectrom.* 234 (2004) 1.
- [34] K.M. Keller, J.M. Zhang, L. Oehlers, J.S. Brodbelt, *J. Am. Soc. Mass Spectrom.* 40 (2005) 1362.
- [35] K. Fukui, Y. Naito, Y. Akiyama, K. Takahashi, *Int. J. Mass Spectrom.* 235 (2004) 25.
- [36] A.T. Iavarone, K. Paech, E.R. Williams, *Anal. Chem.* 76 (2004) 2231.
- [37] J. Wu, S.A. McLuckey, *Int. J. Mass Spectrom.* 237 (2004) 197.